Chapter 7: Paper 2

In this chapter, the paper: "Impaired DNA repair and genomic stability in hereditary tyrosinemia type 1." is presented. The paper contains results from sections 5.2 and 5.3. The paper was published in *GENE*.

~

Gene 495 (2012) 56–61

Contents lists available at SciVerse ScienceDirect

Gene

journal homepage: www.elsevier.com/locate/gene

Short Communication

Impaired DNA repair and genomic stability in hereditary tyrosinemia type 1

E. van Dyk *, P.J. Pretorius

Centre for Human Metabonomics, School for Physical and Chemical Sciences, North-West University, Potchefstroom, 2520, South Africa

ARTICLE INFO

Article history:
Accepted 6 December 2011
Available online 23 December 2011

Keywords:
Hereditary tyrosinemia
Microsatellite instability
Gene expression
Genetic instability
Hepatocellular carcinoma

ABSTRACT

The autosomal recessive disorder, hereditary tyrosinemia type 1 (HT1), is caused by a defective fumarylacetoacetate hydrolase enzyme. Consequently intermediate metabolites such as fumarylacetoacetate, succinylacetone and p-hydroxyphenylpyruvic acid accumulate. Characteristic to HT1 is the development of hepatocellular carcinoma, irrespective of dietary intervention or pharmacological treatment. Carcinogenesis may occur through a chromosomal instability mutator phenotype or a microsatellite instability phenotype, and deficient DNA repair may be a contributing factor thereof. The purpose of this study was to investigate the expression of DNA repair proteins, and the possible occurrence of microsatellite instability in HT1. Gene expression analyses show low expression of *hOGG1* and *ERCC1* in HT1 patient lymphocytes. Results from microsatellite instability analyses show allelic imbalance on chromosome 7 of the *fah*$^{-/-}$ mouse genome, and instability of the D2S123, D5S346 and (possibly) D17S250 microsatellite markers, in HT1 patient lymphocytes.

1. Introduction

A defective fumarylacetoacetate hydrolase (FAH, E.C. 3.1.7.2; GenBank ID: 2184), the last enzyme of the tyrosine degradation pathway, results in the autosomal recessive disorder, Hereditary Tyrosinemia type 1 (HT1, OMIM ID: 276700) (Mitchell et al., 2001). Consequently intermediate metabolites such as fumarylacetoacetate (FAA), maleylacetoacetate (MAA), succinylacetone (SA), p-hydroxyphenylpyruvic acid (pHPPA), p-hydroxyphenylacetic acid (pHPAA) and p-hydroxyphenyllactic acid (pHPLA) accumulate (Mitchell et al., 2001; Sniderman King et al., 2008).

It was previously shown that these metabolites have detrimental effects on the cell. For instance, the pathognomonic metabolite, SA, reacts non-enzymatically with the lysine residue in the active site of DNA ligase, thereby inhibiting the enzyme. This inhibition leads to the slow rejoining of Okazaki fragments (Manabe et al., 1985; Prieto-Alamo and Laval, 1998). pHPPA impairs the base- and nucleotide excision repair capacity of cells by affecting the initiating proteins in these pathways (van Dyk and Pretorius, 2005; van Dyk et al., 2010). The BER capacity of a cell is strongly correlated to the expression of *hOGG1* (GenBank ID: 4968), the glycosylase involved in the initial steps of BER (Christmann et al., 2003; Hodges and Chipman, 2002; Lee et al., 2004). In the same manner, the NER capacity of a cell is strongly correlated to the expression of *ERCC1* (GenBank ID: 2067), the protein involved in the 5′ incision step of NER (Christmann et al., 2003; Langie et al., 2007; Vogel et al., 2000). However, up to now, it has not been reported how the expression of these proteins are affected in HT1 patients.

Furthermore, the intermediate metabolite immediately upstream of FAH, FAA, activates signals such as ERK and the AKT survival pathway, induces apoptosis, and causes endoplasmic reticulum stress (Bergeron et al., 2006; Jorquera and Tanguay, 1999, 2001; Kubo et al., 1998; Orejuela et al., 2008).

Characteristic to HT1 is the development of hepatocellular carcinoma (HCC), irrespective of dietary intervention or pharmacological treatment (Grompe et al., 1998; Grompe, 2001; Mitchell et al., 2001). Instability of the genome is a frequent event in carcinogenesis (Charames and Bapat, 2003; Jackson and Loeb, 2001; Mitra et al., 2002).

Genomic instability can broadly be divided into chromosomal instability and microsatellite instability (Charames and Bapat, 2003). Chromosomal instability refers to the mis-segregation of genetic information, whereas microsatellite instability (MSI) refers to the addition or subtraction of the repeat sequences of microsatellites (Buhard et al., 2006; Charames and Bapat, 2003). MSI is distinct from allelic imbalance and observed loss of heterozygosity (Boland et al., 1998). It was suggested that cancer develops through either a chromosomal

Abbreviations: 18S, *18S* rRNA; BER, base excision repair; cDNA, DNA complementary to RNA; CIN, chromosomal instability mutator phenotype; Creat, creatinine; DNA, deoxyribonucleic acid; DNMT1, DNA methyltransferase 1; dNTP, deoxyribonucleotide triphosphate; DTT, dithiothreitol; EDTA, ethylenediamine tetraacetic acid; *ERCC1*, excision repair cross complementing 1; ERK, Extra cellular signal-regulated protein kinase; FAA, fumarylacetoacetate; FAH, fumarylacetoacetate hydrolase; *gas2*, growth arrest specific 2; HCC, hepatocellular carcinoma; *hOGG1*, human 8-oxoguanine glycosylase; HT1, hereditary tyrosinemia type 1; MAA, maleylacetoacetate; MIN, microsatellite instability mutator phenotype; MMLV, Moloney Murine Leukemia Virus Reverse Transcriptase; MSI, microsatellite instability; NER, nucleotide excision repair; NTBC, 2-(2-nitro-4-trifluoromethylbenzoyl)-1,3-cyclohexanedione; PBS, phosphate buffered saline; PCR, polymerase chain reaction; pHPAA, *para*-hydroxyphenylacetic acid; pHPLA, *para*-hydroxyphenyllactic acid; pHPPA, *para*-hydroxyphenylpyruvic acid; Ref, reference; RNA, ribonucleic acid; rRNA, ribosomal RNA; SA, succinylacetone.

* Corresponding author at: Centre for Human Metabonomics, School for Physical and Chemical Sciences, North-West University, Potchefstroom Campus, Private Bag X6001, Potchefstroom 2520, South Africa. Tel.: +27 18 299 2307; fax: +27 18 293 5248.
E-mail address: Etresia.VanDyk@nwu.ac.za (E. van Dyk).

0378-1119/$ – see front matter © 2012 Elsevier B.V. All rights reserved.
doi:10.1016/j.gene.2011.12.021

instability mutator phenotype (CIN) or a microsatellite instability phenotype (MIN), and the choice is driven by the type of carcinogen (Bardelli et al., 2001; Breivik and Gaudernack, 1999). However, Trautmann et al. (2006) have shown that CIN and MIN are not mutually exclusive in colon cancer. Several reports have shown the presence of chromosomal instability, i.e. chromosomal breakage, aneuploidy, spindle disturbances and segregational defects, in HT1 (Gilbert-Barness et al., 1990; Jorquera and Tanguay, 2001; Zerbini et al., 1992). However, to the best of our knowledge, no MSI has been reported in HT1.

2. Materials and methods

2.1. Patients

Whole blood samples from two female sibling HT1 patients, aged 4 years 10 months, and 1 year 3 months respectively were used in this study. Both patients were referred by a paediatrician to the Potchefstroom Laboratory for Inborn Errors of Metabolism at North-West University (Potchefstroom Campus), South Africa for biochemical diagnosis. Informed consent from the relevant parties concerned and ethical approval by the NWU Ethics Committee (NWU-00096-08-A1) were obtained for the use of these samples. Patient A had severe general amino aciduria, with abnormally elevated urinary tyrosine (305.4 mmol/mol creat; ref. 12–52 mmol/mol creat), methionine (267.4 mmol/mol creat; ref. 6–22 mmol/mol creat), and phenylalanine (273.9 mmol/mol creat; ref. 7–28 mmol/mol creat), as well as increased urinary pHPPA, pHPLA, pHPAA and succinylacetone (263.67 mg/g creat; ref. <0). Follow-up urinary and serum samples showed still elevated urinary tyrosine, methionine, phenylalanine, pHPPA, pHPLA, pHPAA and succinylacetone (187.5 mg/g; ref. <0); and high to high–normal serum tyrosine (165 μmol/l; ref. 19–119 μmol/l), methionine (291 μmol/l; ref. 23–43 μmol/l), phenylalanine (97.4 μmol/l; ref. 26–98 μmol/l). Patient B had high-normal levels of urinary tyrosine (50.15 mmol/mol creat; ref. 6–55 mmol/mol creat), methionine (12.42 mmol/mol creat; ref. 7–27 mmol/mol creat), and phenylalanine (23.51 mmol/mol creat; ref. 4–32 mmol/mol creat), as well as elevated urinary pHPPA, pHPLA, pHPAA and succinylacetone (10.91 mg/g creat; ref. <0). The level of the amino acids in the serum was high, i.e. tyrosine (182 μmol/l; ref. 19–119 μmol/l), methionine (57.5 μmol/l; ref. 23–43 μmol/l), and phenylalanine (106 μmol/l; ref. 26–98 μmol/l).

2.2. FAH deficient mice

Markus Grompe (Oregon Health Sciences University, Portland, OR, USA), kindly provided us with FAH deficient mice (Grompe et al., 1993). In these mice, the FAH deficiency is the result of knockout of the *fah* gene. For breeding purposes the neonatally lethal phenotype can be rescued by administration of NTBC. NTBC inhibits the 4-hydroxyphenylpyruvic acid dioxygenase upstream of FAH, which prevents the accumulation of toxic metabolites such as fumarylacetoacetate. Withdrawal of NTBC causes liver injury in the FAH deficient mice, and death ensues 4–8 weeks later (Duncan et al., 2009).

2.3. RNA and DNA isolation

DNA was extracted from non-cancerous livers of 3 month old control and *fah*$^{-/-}$ mice continuously on NTBC or off NTBC for 40 days. DNA extraction was performed in Oregon (Oregon Health Sciences University, Portland, OR, USA) by Raymond Hickey, with the DNeasy® Tissue kit from Qiagen, according to manufacturer's instructions.

EDTA whole blood samples were obtained for DNA isolation from the whole blood of the healthy control subjects and the HT1 patients and were performed with the FlexiGene DNA kit from Qiagen according to manufacturer's instructions. For RNA extraction, leukocytes were isolated from the blood samples. Briefly, 2 ml of the EDTA treated whole blood was layered on top of 2 ml cold Histopaque® in a 15 ml centrifuge tube. The samples were then centrifuged for 15 min at 550 *g*. The plasma layer was discarded, and the buffy coat transferred to a 1.5 ml microcentrifuge tube. To this, 1 ml PBS was added. The samples were briefly vortexed and then centrifuged for 3 min at 1100 *g*. The supernatant was discarded, and RNA isolated from the cell pellets with the Nucleospin RNAII kit (Macherey-Nagel) according to the manufacturer's specifications.

2.4. cDNA synthesis

cDNA was synthesised from extracted RNA using the MMLV high performance reverse transcriptase cDNA synthesis kit (Epicentre® Biotechnologies). For each reaction (reaction volume: 10 μl), 1.5 μg RNA, 1 μl oligo dT primer (10 μM), 1 μl *18S* rRNA reverse primer (10 μM) and PCR grade water were mixed. The reactions were incubated for 2 min at 65 °C, whereafter the reactions were placed on ice for 5 min. In the meantime, 2 μl MMLV reaction buffer (10×), 2 μl DTT (0.1 M), 3 μl HPLC grade water, 2 μl dNTP mix (10 mM of each dNTP; New England Biolabs®), 0.5 μl RNasin® (40 U/μl; Promega), and 0.5 μl MMLV (200 U/μl) were mixed. Of this mixture, 10 μl was added to each reaction. The reactions were then placed overnight at 37 °C in an Eppendorf® thermal cycler. The cDNA synthesis was terminated by increasing the incubation temperature to 85 °C for 5 min. The samples were stored at 4 °C.

2.5. Real-time quantitative PCR

All cDNA samples were diluted 250× with PCR grade water. Reaction mixtures for all gene expression assays contained: 10 μl Taqman mastermix (2×; Applied Biosystems™; part # 4364341), 1 μl *18S* primer/probe mix, 1 μl gene of interest primer/probe mix and 6 μl PCR grade water. To each reaction, 2 μl of the diluted cDNA was added. All samples were assayed in triplicate. The real-time PCR program was set to 95 °C for 10 min and then 40 cycles of 95 °C for 15 s and 60 °C for 1 min (fluorescence reading). All real-time PCR data were analysed with 7500 System SDS software version 2.0.5 from Applied Biosystems™.

2.6. Microsatellite instability assay

A panel of four microsatellite markers (D3Mit21, D7Mit18, D7Mit10 and D11Mit7) (Supplementary Table 1) as described by Zhang et al. (Zhang et al., 2004), was used to examine microsatellite instability in DNA extracted from the *fah*$^{-/-}$ mouse livers. A panel of five microsatellite markers (Supplementary Table 2), as suggested by the National Cancer Institute workshop in 1997 (Boland et al., 1998), was used to analyse microsatellite instability in the HT1 patients. The microsatellite markers used included two mononucleotide repeats: BAT25, BAT26, and three dinucleotide repeats: D5S346, D2S123, and D17S250. Primer sequences for all markers are given in Supplementary Table 3.

All microsatellite analyses proceeded according to the same basic protocol, i.e. DNA amplification by PCR on a Biometra thermocycler (Biometra, Germany), PCR product confirmation by gel electrophoresis on a 2% agarose gel and microsatellite analysis with an Agilent 2100 Bioanalyzer (Odenthal et al., 2009). All PCR reactions were performed with the KAPA HiFi™ PCR kit from KAPABIOSYSTEMS. PCR reactions for the human microsatellite analyses, contained: 5 μl Fidelity buffer (5×), 0.5 μl dNTPS (10 mM of each dNTP), 0.5 μl of each primer (10 μM), 1.5 μl $MgCl_2$ (25 mM), 300 ng DNA, 0.5 μl KAPA HiFi polymerase (1 U/μl), and PCR grade water up to 25 μl. Thermocycling conditions were: 95 °C for 2 min, followed by 25 cycles of 98 °C for 20 s, Tm for 15 s, and 68 °C for 20 s, and a final extension step of 68 °C for 1 min. PCR products were stored at 4 °C until further use.

The PCR reaction mixtures for studying the mouse microsatellites contained: 3 μl GC buffer (5×), 0.3 μl dNTPs (10 mM of each dNTP), 300 ng DNA, 0.3 μl of each primer (10 μM), 0.6 μl $MgCl_2$ (25 mM), 0.3 μl KAPA HiFi polymerase (1 U/μl), and PCR grade water up to 15 μl. Thermocycling conditions were: 95 °C for 6 min followed by 15 cycles of 98 °C for 20 s, 63 °C for 30 s (decreased by 0.5 °C each cycle), 68 °C for 20 s, and then 25 cycles of 98 °C for 20 s, 58 °C for 30 s, and 68 °C for 20 s, with a final extension of 68 °C for 5 min. PCR products were stored at 4 °C until use.

After confirmation of successful PCR by means of electrophoresis on a 2% agarose gel, 1 μl of each PCR product was analysed on an Agilent DNA 1000 chip with the Agilent 2100 Bioanalyzer according to the manufacturer's instructions. Briefly, the gel–dye mix was prepared by equilibrating the DNA dye concentrate and DNA gel matrix to room temperate for 30 min. After equilibration, 25 μl of the DNA dye concentrate was added to the vial DNA gel matrix. The gel–dye mix was vortexed and briefly centrifuged. After the gel–dye mix was transferred to the spin filter, it was centrifuged for 15 min at 2240 *g*. Between uses, the gel–dye mix was stored at 4 °C.

For each analysis the gel–dye mix was equilibrated to room temperature. The DNA 1000 chip was primed by adding 9 μl DNA gel matrix to the assigned well and applying pressure for 1 min with the plunger of the chip priming station at 1 ml. Another 9 μl gel–dye mix was added to each of the next two assigned wells. Then 5 μl marker was added to all 12 sample wells and the ladder well. Of each sample, 1 μl was added to a separate well and 1 μl DNA ladder was added to the ladder well. The DNA 1000 chip was then vortexed for 1 min at 2400 rpm. Within 5 min the DNA 1000 chip was run on the Agilent 2100 Bioanalyzer. Results were processed with Agilent 2100 expert software version B.02.03.SI307.

3. Results and discussion

It was previously shown that the HT1 metabolites, SA and pHPPA, decrease the ability of cells for base- and nucleotide excision repair (van Dyk et al., 2010). However, currently no information is available on the expression levels of DNA repair proteins in HT1 patients. In view of the fact that the expression levels of *hOGG1* and *ERCC1* are closely correlated with the BER and NER capacity of cells (Hodges and Chipman, 2002; Langie et al., 2007; Lee et al., 2004; Vogel et al., 2000), the level of expression of *hOGG1* and *ERCC1* was assessed in the HT1 patients. Results of the expression of *hOGG1* and *ERCC1* in the control person and each of the patients are given in Fig. 1.

The expression of *hOGG1* and *ERCC1* is low in both patients. Compared to expression of *hOGG1* control cells, expression of the gene is approximately 53% in patient A and 8% in patient B. The relative expression of *ERCC1* follows the same trend, with patient A having approximately 43% expression and patient B 12% expression. The reduction of *hOGG1* and *ERCC1* to approximately the same levels in each patient, is consistent with the observation by Vogel et al. (2002) that the mRNA levels of these genes are closely correlated. They speculated that *hOGG1* and *ERCC1* might be regulated by the same factors (Vogel et al., 2002).

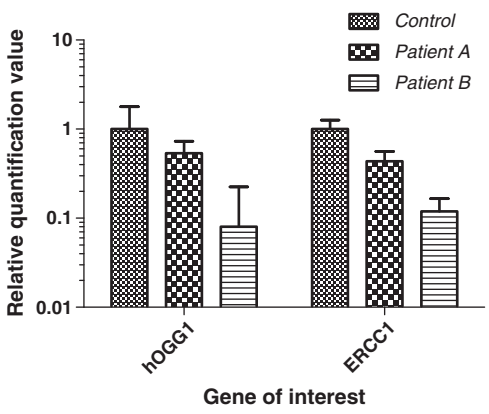

Fig. 1. Expression of *hOGG1* and *ERCC1* by control and patient primary lymphocytes. Due to limited sample availability, relative quantification values are mean values for 3 technical repeats. Error bars represent standard deviation.

The low expression of *hOGG1* and *ERCC1* in HT1 patients, coupled with the effect of accumulating metabolites on the protein functionality of BER and NER proteins (van Dyk et al., 2010), suggests that the capacity of HT1 cells for DNA repair is severely affected. Not only is the expression of the repair proteins low, but also the functionality of the proteins that are expressed are diminished by the accumulating metabolites (van Dyk et al., 2010). This diminished capacity for DNA repair may contribute to the development of HCC in HT1.

It was suggested by Loeb that microsatellite instability is a marker of a mutator phenotype in cancer, and that deficiency of DNA repair is one of the contributing factors to the development of the mutator phenotype (Loeb, 1994). Therefore, the observed decreased DNA repair capacity in HT1 cells, prompted an investigation into the occurrence of MSI in HT1.

DNA samples from control and *fah*$^{-/-}$ mice were investigated. FAH deficient mice were either continuously treated with NTBC or NTBC treatment were withdrawn for 40 days. Although 40 days seem limiting, it was reported that this time interval was enough to elicit an endoplasmic reticulum stress response (Bergeron et al., 2006), and cause progressive liver and kidney pathophysiology (Orejuela et al., 2008). Microsatellite markers as described by Zhang et al. (2004)) were used to determine microsatellite instability because they found that genomic instability in mouse chromosomes 3, 7, 11 and 16 have a role in the development and progression of HCC in mice.

The results of the MSI analyses, after amplification of markers by conventional PCR and separation of the amplicons on a DNA 1000 chip from Agilent on a 2100 Bioanalyzer, are given in Fig. 2.

Similar microsatellite amplification patterns were obtained for each of the microsatellite markers when comparing the microsatellite amplification pattern in the control and the *fah*$^{-/-}$ mice. The only slight difference that can be observed, is in the amplification profile of D7Mit18. In the control the intensity of the largest fragment (204 bp) is the highest, with the three smaller fragments (131, 156, 163 bp) having comparable intensities. In both of the *fah*$^{-/-}$ mice the smallest (131 bp) and largest (204 bp) fragments have similar intensities, with the two mid-sized fragments (156 and 163 bp) at a much lower intensity. This change may be the result of allelic imbalance occurring. Allelic imbalance is a molecular level characteristic feature of chromosomal imbalance, which is a regular trait in tumours such as HCC (Aihara et al., 1998; Zhang et al., 2004). It was suggested that chromosomes 3, 7, and 11 carry tumour suppressor genes (Zhang et al., 2004). Although the sample size is small, the observed change in intensity of the D7Mit18 fragments could be an indicator of chromosomal imbalance and may point to the development of HCC in the *fah*$^{-/-}$ mice, which would be in line with the observations by Al-Dhalimy et al. that HCC develops in *fah* deficient mice even with dietary intervention and pharmacological treatment (Al-Dhalimy et al., 2002; Mitchell et al., 2001). Even though these MSI analyses have not shown microsatellite instability, the possibility of MSI occurring in the genome of the *fah*$^{-/-}$ mice can not be excluded. As the occurrence of chromosomal instability shows that genetic instability does occur in *fah* deficient mice, a more extensive panel of microsatellite markers might reveal microsatellite instability.

The stability of microsatellite DNA in HT1 patients was also assessed by MSI analysis. Since the expression level of DNA repair proteins was low in lymphocytes of HT1 patients, the reduced DNA repair capacity in these cells may result in MSI in the lymphocytes. In individuals of Eurasian origin, BAT25 and BAT26 are quasimonomorphic, i.e. small size differences of no more than 1 or 2 basepairs

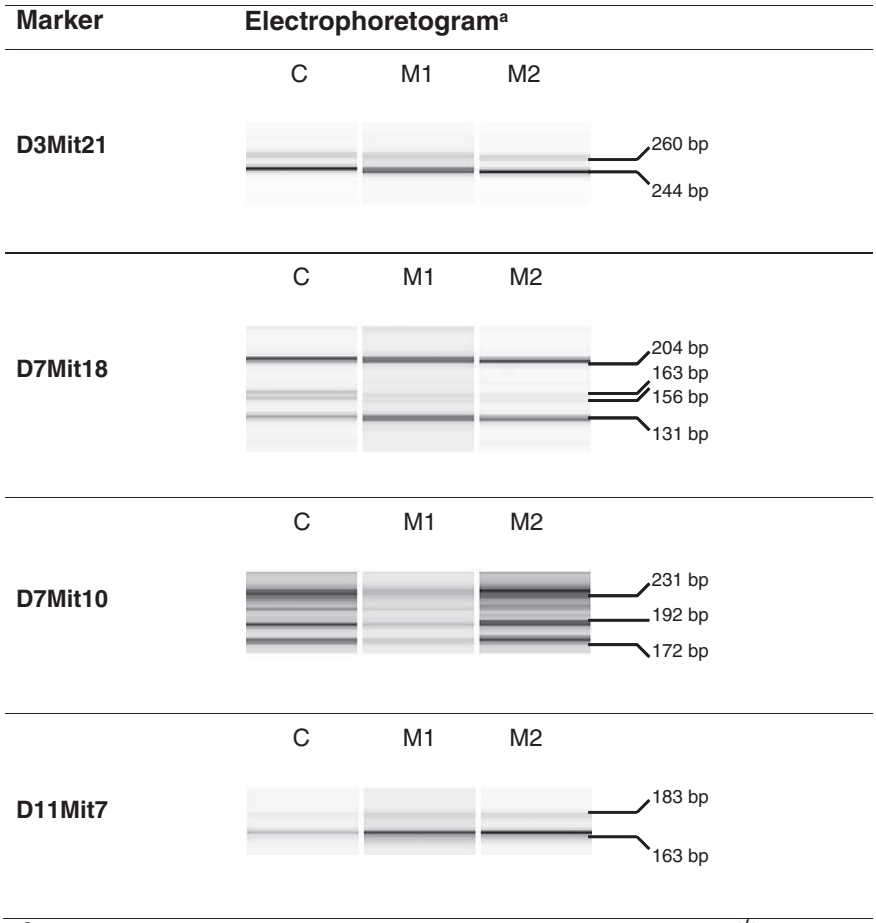

[a] For each marker the amplicon band sizes decreases from top to bottom. C: *fah*$^{+/+}$ control mouse; M1: *fah*$^{-/-}$ mouse constantly on NTBC; M2: *fah*$^{-/-}$ mouse off NTBC for 40 days.

Fig. 2. Microsatellite analysis of mouse DNA.

occur (Buhard et al., 2006), making direct comparison between control and patient samples possible. However, dinucleotide repeats, such as CA repeats may have different alleles in a population (Richards and Hawley, 2011). More than one control person was therefore included in the study to compensate for inter-individual variability that may exist in the dinucleotide repeats. The microsatellite analysis results after separation on a DNA 1000 chip is given in Fig. 3.

From this result it is evident that both of the mononucleotide repeats, BAT25 and BAT26, show no variance between patient and control samples i.e. the microsatellite amplification pattern is the same. Similar amplification patterns of D2S123 are also observed for the controls and patient B. (Although the larger bands of approximately 313 and 324 bp are not clearly visible in control 1, the bands are present). For patient A, however, a slightly altered amplification pattern is observed. Similar to controls 1 and 2 and patient B, bands of approximately 234, 260, 280, 290 bp are seen in patient A, but the 313 and 324 bp bands are absent. Instead a large band of 363 bp is seen. Unlike in the controls and patient B, where the smallest bands are the most prominent, in patient A the largest band is the most prominent.

The microsatellite amplification pattern of the dinucleotide D5S346, is similar for controls 1 and 2 and patient A. Bands of approximately 126 and 136 bp are present. In patient B, this microsatellite amplification profile is slightly different with bands of 126, 136, and 188 basepairs.

The D17S250 dinucleotide repeat shows the largest variation in the microsatellite amplification pattern. Although the amplification bands are slightly smaller in control 2 compared to control 1, the same pattern is observed. For both controls, six bands can be distinguished, with the largest and smallest bands being the most prominent. When compared to the controls, the microsatellite amplification pattern of D17S250 is different in the patients. In both patient A and patient B, only four amplification bands are present. Furthermore, unlike the controls, in the patients the two smallest bands have the highest intensity.

Interestingly, when comparing patient A to patient B, different amplification patterns were obtained for the D2S123 and D5S346 dinucleotide repeats, but a similar pattern was obtained for the D17S250 dinucleotide repeat. Keeping in mind that the two HT1 patients are sisters and that sequence length variation, i.e. microsatellite DNA, is inherited in a co-dominant Mendelian way (Srikwan et al., 1996) and since the D2S123 marker pattern of patient B is similar to the controls, it suggests that the altered pattern seen in patient A is novel to patient A and not inherited. Similarly, the altered pattern of D5S346 in patient B might be novel to patient B. The similarity of the microsatellite amplification pattern of D17S250 between the patients, but difference to the microsatellite amplification pattern obtained for the controls, could be novel microsatellite instability in both of the patients, but may also be because of the high degree of allele variability that exists for dinucleotide repeats (Richards and Hawley, 2011). Like the results obtained with the D7Mit18 marker suggest possible allelic imbalance in the *fah* deficient mice, the fragment intensity changes seen with the D17S250 marker in the patients, may also reflect allelic imbalance. However, as it is not clear whether the D17S250 MSI in the HT1 patients is due to novel

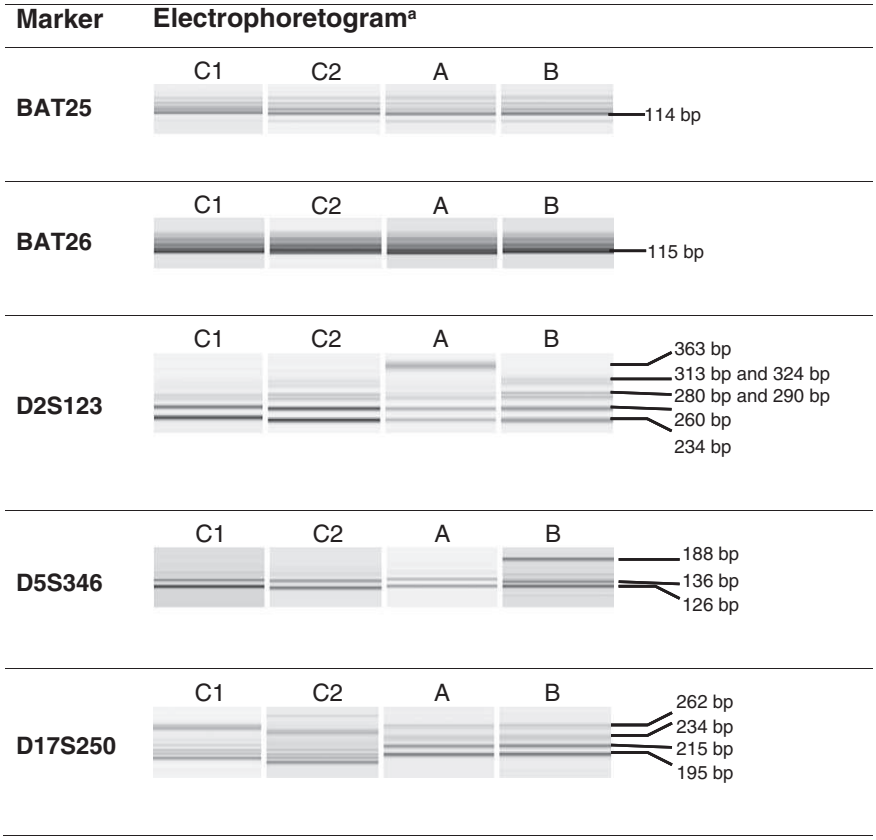

[a] For each marker the amplicon band sizes decreases from top to bottom. C1: controlsubject 1; C2: control subject 2; A: Patient A; B: Patient B

Fig. 3. Microsatellite analysis with the five microsatellite markers as recommended by the Bethesda panel.

microsatellite instability or because of the mentioned high allele variability for dinucleotides, it is difficult to ascertain whether the D17S250 intensity changes observed in the patients are truly due to allelic imbalance. These results, nonetheless, show that microsatellite instability occurs in the lymphocytes of these two HT1 patients.

Tumours are regarded as MSI-H (high frequency of MSI) when two or more of the microsatellite markers show instability, MSI-L (low frequency of MSI) when one of the markers show instability and MSS when no instability is found (Boland et al., 1998). Although the microsatellites analysed in the patients were from non-tumour DNA, it is interesting to note that if the above mentioned criteria for tumour MSI classification is used, both patients would be classified as MSI-L, and possibly even MSI-H, as instability is observed for one (maybe two) of the five markers tested.

Several reports have described microsatellite instability analyses as a useful method to determine defective DNA mismatch repair (Buhard et al., 2006; Dietmaier et al., 1997; House et al., 2003; Macdonald et al., 1998; Maehara et al., 2001). The presence of MSI in the lymphocytes of the HT1 patients, therefore, albeit indirectly, suggests that in addition to the decreased capacity for base- and nucleotide repair by HT1 cells (van Dyk et al., 2010), the capacity of HT1 cells for DNA mismatch repair may be affected.

4. Conclusion

Even though a small number of samples were used, the results should not be overlooked as it may form the basis for future research. The first reports on chromosomal instability and aneuploidy in HT1 were made after observations with limited sample numbers, i.e. three HT1 patients and one HT1 patient, respectively (Gilbert-Barness et al., 1990; Zerbini et al., 1992).

Our results have shown the presence of allelic imbalance on chromosome 7 of the *fah*$^{-/-}$ mouse genome, confirming previously reported chromosomal instability in HT1 (Gilbert-Barness et al., 1990; Jorquera and Tanguay, 2001; Zerbini et al., 1992). Incidentally, our observation of instability of specifically the D7Mit18 microsatellite marker, also indicates the possible involvement of the growth arrest specific 2 (*gas2*) and *ras* genes in HT1. The D7Mit18 marker is located in the *gas2* gene, and according to the Entrez gene summary, high levels of this gene are associated with growth arrested cells. Instability of this gene could therefore be one of the contributing factors of the cell cycle arrest seen in HT1 (Bergeron et al., 2006; Vogel et al., 2004). At the same time, D7Mit18 is located 1.9 cM from *ras* (Zhang et al., 2004), a cancer associated gene (Lumniczky et al., 1998), suggesting the possible involvement of *ras* in the development of HCC in HT1.

Our results furthermore showed instability of the D2S123, D5S346 and possibly the D17S250 microsatellite markers of the two HT1 patient studied. Given that DNA repair deficiency may result in relaxed genome stability (Loeb, 1994), it is possible that the observed low expression of the DNA repair proteins (and by extension, a decreased DNA repair capacity) may be a contributing factor to the observed genetic instability seen in the lymphocytes of the HT1 patients. In the liver of HT1 patients, the same type of situation may occur, only more severe. In HT1 hepatocytes, the presence of FAA which is highly mutagenic (Jorquera and Tanguay, 1997), may place an additional burden on the already decreased DNA repair capacity. As these HT1 cells are also resistant to cell death (Orejuela et al., 2008), mutations may accumulate. These accumulated mutations may then contribute to the development of HCC.

In conclusion, our results have shown that in the studied HT1 patients the expression of DNA repair proteins, hOGG1 and ERCC1, are

low, and that microsatellite instability is present. The development of HCC in HT1 may therefore not be only as a result of chromosomal instability, but also because of microsatellite instability. Also, the decreased DNA repair capacity in HT1 cells may be a contributing factor of the observed genomic instability.

Supplementary materials related to this article can be found online at doi:10.1016/j.gene.2011.12.021.

Acknowledgments

The authors would like to extend a very grateful thank you to the following persons:

- Markus Grompe (Oregon Health Sciences University, Portland, OR, USA), for providing us with the FAH deficient mice,
- Raymond Hickey (Oregon Health Sciences University, Portland, OR, USA), for performing DNA extractions from the livers of the FAH deficient mice, and critical reading of the manuscript,
- Japie Mienie (Potchefstroom Laboratory for Inborn Errors of Metabolism at North-West University (Potchefstroom Campus), South Africa), for providing us with whole blood samples from the two HT1 patients.

The authors would also like to thank the National Research Foundation (NRF South Africa) for the financial support towards the research conducted for this paper.

References

Aihara, T., Noguchi, S., Miyoshi, Y., Nakano, H., Sasaki, Y., Nakamura, Y., Monden, M., Imaoka, S., 1998. Allelic imbalance of insulin-like growth factor II gene expression in cancerous and precancerous lesions of the liver. Hepatology 28 (1), 86–89.

Al-Dhalimy, M., Overturf, K., Finegold, M., Grompe, M., 2002. Long-term therapy with NTBC and tyrosine-restricted diet in a murine model of hereditary tyrosinemia type I. Mol. Genet. Metab. 75 (1), 38–45.

Bardelli, A., Cahill, D.P., Lederer, G., Speicher, M.R., Kinzler, K.W., Vogelstein, B., Lengauer, C., 2001. Carcinogen-specific induction of genetic instability. Proc. Natl. Acad. Sci. 98 (10), 5770–5775.

Bergeron, A., Jorquera, R., Orejuela, D., Tanguay, R.M., 2006. Involvement of endoplasmic reticulum stress in hereditary tyrosinemia type I. J. Biol. Chem. 281 (9), 5329–5334.

Boland, C.R., Thibodeau, S.N., Hamilton, S.R., Sidransky, D., Eshleman, J.R., Burt, R.W., Meltzer, S.J., Rodriguez-Bigas, M.A., Fodde, R., Ranzani, G.N., Srivastava, S., 1998. A National Cancer Institute Workshop on Microsatellite Instability for cancer detection and familial predisposition: development of international criteria for the determination of microsatellite instability in colorectal cancer. Cancer Res. 58 (22), 5248–5257.

Breivik, J., Gaudernack, G., 1999. Genomic instability, DNA methylation, and natural selection in colorectal carcinogenesis. Semin. Cancer Biol. 9 (4), 245–254.

Buhard, O., Cattaneo, F., Wong, Y.F., Yim, S.F., Friedman, E., Flejou, J., Duval, A., Hamelin, R., 2006. Multipopulation analysis of polymorphisms in five monomucleotide repeats used to determine the microsatellite instability status of human tumors. J. Clin. Oncol. 24 (2), 241–251.

Charames, G.S., Bapat, B., 2003. Genomic instability and cancer. Curr. Mol. Med. 3 (7), 589–596.

Christmann, M., Tomicic, M.T., Roos, W.P., Kaina, B., 2003. Mechanisms of human DNA repair: an update. Toxicology 193 (1–2), 3–34.

Dietmaier, W., Wallinger, S., Bocker, T., Kullman, F., Fishel, R., Ruschoff, J., 1997. Diagnostic microsatellite instability: definition and correlation with mismatch repair protein expression. Cancer Res. 57, 4749–4756.

Duncan, A.W., Hickey, R.D., Paulk, N.K., Culberson, A.J., Olson, S.B., Finegold, M.J., Grompe, M., 2009. Ploidy reductions in murine fusion-derived hepatocytes. PLoS Genet. 5 (2), e1000385.

Gilbert-Barness, E., Barness, L.A., Meisner, L.F., 1990. Chromosomal instability in hereditary tyrosinemia type I. Pediatr. Pathol. 10 (1–2), 243–252.

Grompe, M., 2001. The pathophysiology and treatment of hereditary tyrosinemia type 1. Semin. Liver Dis. 21 (4), 563–571.

Grompe, M., al-Dhalimy, M., Finegold, M., Ou, C.N., Burlingame, T., Kennaway, N.G., Soriano, P., 1993. Loss of fumarylacetoacetate hydrolase is responsible for the neonatal hepatic dysfunction phenotype of lethal albino mice. Genes Dev. 7 (12A), 2298–2307.

Grompe, M., Overturf, K., Al-Dhalimy, M., Finegold, M., 1998. Therapeutic trials in the murine model of hereditary tyrosinemia type 1: a progress report. J. Inherit. Metab. Dis. 21, 518–531.

Hodges, N.J., Chipman, J.K., 2002. Down-regulation of the DNA-repair endonuclease 8-oxo-guanine DNA glycosylase 1 (hOGG1) by sodium dichromate in cultured human A549 lung carcinoma cells. Carcinogenesis 23 (1), 55–60.

House, M.G., Herman, J.G., Guo, M.Z., Hooker, C.M., Schulick, R.D., Cameron, J.L., Hruban, R.H., Maitra, A., Yeo, C.J., 2003. Prognostic value of hMLH1 methylation and microsatellite instability in pancreatic endocrine neoplasms. Surgery 134 (6), 902–908.

Jackson, A.L., Loeb, L.A., 2001. The contribution of endogenous sources of DNA damage to the multiple mutations in cancer. Mutat. Res. Fundam. Mol. Mech. Mutagen. 477 (1–2), 7–21.

Jorquera, R., Tanguay, R.M., 1997. The mutagenicity of the tyrosine metabolite, fumarylacetoacetate, is enhanced by glutathione depletion. Biochem. Biophys. Res. Commun. 232 (1), 42–48.

Jorquera, R., Tanguay, R.M., 1999. Cyclin B-dependent kinase and caspase-1 activation precedes mitochondrial dysfunction in fumarylacetoacetate-induced apoptosis. FASEB J. 13 (15), 2284–2298.

Jorquera, R., Tanguay, R.M., 2001. Fumarylacetoacetate, the metabolite accumulating in hereditary tyrosinemia, activates the ERK pathway and induces mitotic abnormalities and genomic instability. Hum. Mol. Genet. 10 (17), 1741–1752.

Kubo, S., Sun, M., Miyahara, M., Umeyama, K., Urakami, K., Yamamoto, T., Jakobs, C., Matsuda, I., Endo, F., 1998. Hepatocyte injury in tyrosinemia type 1 is induced by fumarylacetoacetate and is inhibited by caspase inhibitors. Proc. Natl. Acad. Sci. U. S. A. 95 (16), 9552–9557.

Langie, S.A., Knaapen, A.M., Houben, J.M., van Kempen, F.C., de Hoon, J.P., Gottschalk, R.W., Godschalk, R.W., van Schooten, F.J., 2007. The role of glutathione in the regulation of nucleotide excision repair during oxidative stress. Toxicol. Lett. 168 (3), 302–309.

Lee, M.R., Kim, S.H., Cho, H.J., Lee, K.Y., Moon, A.R., Jeong, H.G., Lee, J.S., Hyun, J.W., Chung, M.H., You, H.J., 2004. Transcription factors NF-YA regulate the induction of human OGG1 following DNA-alkylating agent methylmethane sulfonate (MMS) treatment. J. Biol. Chem. 279 (11), 9857–9866.

Loeb, L.A., 1994. Microsatellite instability: marker of a mutator phenotype in cancer. Cancer Res. 54, 5059–5063.

Lumniczky, K., Antal, S., Unger, E., Wunderlich, L., Hidvegi, E.J., Safrany, G., 1998. Carcinogenic alterations in murine liver, lung, and uterine tumors induced by in utero exposure to ionizing radiation. Mol. Carcinog. 21 (2), 100–110.

Macdonald, G.A., Greenson, J.K., Saito, K., Cherian, S.P., Appelman, H.D., Boland, C.R., 1998. Microsatellite instability and loss of heterozygosity at DNA mismatch repair gene loci occurs during hepatic carcinogenesis. Hepatology 28 (1), 90–97.

Maehara, Y., Oda, S., Sugimachi, K., 2001. The instability within: problems in current analyses of microsatellite instability. Mutat. Res./DNA Repair 461 (4), 249–263.

Manabe, S., Sassa, S., Kappas, A., 1985. Hereditary tyrosinemia. Formation of succinylacetone-amino acid adducts. J. Exp. Med. 162 (3), 1060–1074.

Mitchell, G.A., Grompe, M., Lambert, M., Tanguay, R.M., 2001. Hypertyrosinemia, In: Scriver, C.R., Beaudet, A.L., Sly, W.S., Valle, D. (Eds.), The Metabolic and Molecular Bases of Inherited Disease, 8th edn. McGraw-Hill, New York, pp. 1777–1806.

Mitra, S., Izumi, T., Boldogh, I., Bhakat, K.K., Hill, J.W., Hazra, T.K., 2002. Choreography of oxidative damage repair in mammalian genomes. Free Radic. Biol. Med. 33 (1), 15–28.

Odenthal, M., Barta, N., Lohfink, D., Drebber, U., Schulze, F., Dienes, H.P., Baldus, S.E., 2009. Analysis of microsatellite instability in colorectal carcinoma by microfluidic-based chip electrophoresis. J. Clin. Pathol. 62 (9), 850–852.

Orejuela, D., Jorquera, R., Bergeron, A., Finegold, M.J., Tanguay, R.M., 2008. Hepatic stress in hereditary tyrosinemia type 1 (HT1) activates the AKT survival pathway in the fah$^{-/-}$ knockout mice model. J. Hepatol. 48 (2), 308–317.

Prieto-Alamo, M.J., Laval, F., 1998. Deficient DNA-ligase activity in the metabolic disease tyrosinemia type I. Proc. Natl. Acad. Sci. U. S. A. 95 (21), 12614–12618.

Richards, J.E., Hawley, R.S., 2011. The Human Genome: A User's Guide, 3rd ed. Academic Press, London, U.K.

Sniderman King, L., Trahms, C., Scott, C.R., 2008. Tyrosinemia type 1Available: http://www.ncbi.nlm.nih.gov/bookshelf/br.fcgi?book=gene&part=tyrosinemia[2010, October].

Srikwan, S., Field, D., Woodruff, D.S., 1996. Genotyping free-ranging rodents with heterologous PCR primer pairs for hypervariable nuclear microsatellite loci. J. Sci. Soc. Thail. 22, 267–274.

Trautmann, K., Terdiman, J.P., French, A.J., Roydasgupta, R., Sein, N., Kakar, S., Fridlyand, J., Snijders, A.M., Albertson, D.G., Thibodeau, S.N., Waldman, F.M., 2006. Chromosomal instability in microsatellite-unstable and stable colon cancer. Clin. Cancer Res. 12 (21), 6379–6385.

van Dyk, E., Pretorius, P.J., 2005. DNA damage and repair in mammalian cells exposed to p-hydroxyphenylpyruvic acid. Biochem. Biophys. Res. Commun. 338 (2), 815–819.

van Dyk, E., Steenkamp, A., Koekemoer, G., Pretorius, P.J., 2010. Hereditary tyrosinemia type 1 metabolites impair DNA excision repair pathways. Biochem. Biophys. Res. Commun. 401 (1), 32–36.

Vogel, U., Dybdahl, M., Frentz, G., Nexo, B.A., 2000. DNA repair capacity: inconsistency between effect of over-expression of five NER genes and the correlation to mRNA levels in primary lymphocytes. Mutat. Res. 461 (3), 197–210.

Vogel, U., Moller, P., Dragsted, L., Loft, S., Pedersen, A., Sandstrom, B., 2002. Inter-individual variation, seasonal variation and close correlation of OGG1 and ERCC1 mRNA levels in full blood from healthy volunteers. Carcinogenesis 23 (9), 1505–1509.

Vogel, A., van Den Berg, I.E., Al-Dhalimy, M., Groopman, J., Ou, C.N., Ryabinina, O., Iordanov, M.S., Finegold, M., Grompe, M., 2004. Chronic liver disease in murine hereditary tyrosinemia type 1 induces resistance to cell death. Hepatology 39 (2), 433–443.

Zerbini, C., Weinberg, D.S., Hollister, K.A., Perez-Atayde, A.R., 1992. DNA ploidy abnormalities in the liver of children with hereditary tyrosinemia type I. Correlation with histopathologic features. Am. J. Pathol. 140 (5), 1111–1119.

Zhang, S.H., Cong, W.M., Shi, J.Q., Wei, H., 2004. Genome instability of murine hepatocellular carcinomas with low and high metastatic capacities. World J. Gastroenterol. 10 (4), 521–524.